Relative Motion and the Geometry of Formations in Keplerian Elliptic Orbits*

Prasenjit Sengupta† and Srinivas R. Vadali‡
Texas A&M University, College Station, TX 77843-3141

Abstract

The well-known Hill-Clohessy-Wiltshire equations that are used for the design of formation flight relative orbits are based on a circular reference orbit. Classical solutions such as the projected circular or general circular relative orbit are no longer valid in the presence of eccentricity. This paper studies the effects of eccentricity on relative motion for Keplerian orbits. A new linear condition for bounded motion in relative position coordinates is derived, that is valid for arbitrary eccentricities and epoch of the reference orbit. It is shown that the solutions to the Tschauner-Hempel equations that are used for rendezvous in elliptic orbits are directly related to the description of relative motion using small orbital element differences. A meaningful geometric parameterization for relative motion near a Keplerian elliptic orbit of arbitrary eccentricity is also developed. The eccentricity-induced effects are studied and exploited to obtain desired shapes of the relative orbit. Equations relating these parameters to initial conditions, and differential classical and nonsingular elements are also derived. This parameterization is very useful for the analysis of more complicated models, such as the nonlinear relative motion problem.

Introduction

The study of relative motion between satellites in Keplerian elliptic orbits has been of recent interest from the point of view of designing clusters of spacecraft flying in formation around a planet. Such formations find use in terrestrial observation, communication, and stellar interferometry. Of more recent interest, is the potential of use of such formations in orbits that are highly eccentric. Examples of such missions have been presented by Carpenter

*An earlier version was presented as Paper AAS 06-161 at the 16th AAS/AIAA Spaceflight Mechanics Conference, Tampa, FL, January 2006.

†Research Associate, Department of Aerospace Engineering, MS 3141, prasenjit@tamu.edu, Member, AIAA.

‡Stewart & Stevenson-I Professor, Department of Aerospace Engineering, MS 3141, svadali@aero.tamu.edu, Associate Fellow, AIAA.

et al.[1], that include reference low Earth orbit and highly elliptical orbit missions. The Magnetosphere Multiscale Mission [2] is another example, where the apogee and perigee are of the order of 12-30$R_\oplus$ and 1.2$R_\oplus$, respectively (with $R_\oplus$ denoting the radius of the Earth), yielding eccentricities of the order of 0.8 and higher.

Traditional formation design relies on the study of the Hill-Clohessy-Wiltshire (HCW) equations[3, 4]. This model assumes a circular reference orbit and a linearized differential gravity field based on the two-body problem. Conditions for bounded motion, known as HCW initial conditions, are easily derived for this model and they have found wide applicability for formation flight. The violation of the underlying assumptions of the HCW model leads to deviation from the motion predicted. A large body of literature exists that deals with the violation of the assumptions, either individually, or in various combinations. The effects of nonlinearity in the differential gravity field, have been studied by the use of perturbation techniques, as shown in Refs. [5, 6, 7, 8]. The effects of eccentricity of the reference orbit on the formation have also been studied extensively. Anthony and Sasaki[9] obtained approximate solutions to the HCW equations by including quadratic nonlinearities and first-order eccentricity effects. Second-order eccentricity effects were also accounted for, in Refs. [10, 11], by Hamiltonian modeling of the HCW equations. Vaddi *et al.*[12] studied the combined problem of eccentricity and nonlinearity and obtain periodicity conditions in the presence of these effects. However, these conditions lose validity even for intermediate eccentricities, primarily because of the higher-order coupling between eccentricity and nonlinearity. Inalhan *et al.*[13] obtained a boundedness condition for the linear problem with arbitrary eccentricities, by providing an explicit equation relating the initial conditions at perigee. For all other cases of epoch, the initial conditions can be obtained by matrix operations. Sengupta *et al.*[14] obtained expressions for periodic relative motion by accounting for quadratic nonlinearities, valid for arbitrary eccentricities. Gurfil[15] posed the bounded-motion problem in terms of an energy-matching condition and presented an algorithm for optimal single-impulse formation-keeping. The boundedness condition in Ref. [15] is presented as the solution to a sixth-order polynomial equation in one variable, and is valid for general two-body motion.

State transition matrices that reflect the effect of eccentricity, have also been derived, and are presented in Refs. [16, 17, 18, 19]. Reference [16] used a series expansion for radial distance and true anomaly, in terms of time. However, for moderate eccentricities, the convergence of such series requires the inclusion of higher-order terms. Other state transition matrices are obtained from the Tschauner-Hempel equations[20], and use the true anomaly f as the independent variable, and are therefore implicit in time.

Relative motion can also be characterized by analytically propagating the orbital elements

corresponding to each satellite[21, 22]. In Ref. [21], this is performed in a time-explicit manner, by using a Fourier-Bessel expansion of the true anomaly in terms of the mean anomaly. However, it is shown that for eccentricities of 0.7, terms up to the tenth order in eccentricity are required in the series. In Ref. [22], a methodology has been proposed where Kepler's equation[23] is solved for the Deputy, but is not required for the Chief, if the Chief's true anomaly is used as the independent variable.

Due to the nonlinear mapping between local frame Cartesian coordinates and orbital elements, errors in the Cartesian frame are translated into very small errors in the orbital angles. Thus, linear equations relating relative position and velocity to small orbital element differences have also been obtained, by either obtaining the partials of the former with respect to the latter[24], or by linearizing the direction cosine matrix of the reference frame rotating with the Deputy, with respect to that of the Chief[25]. The linear relationship between relative motion in the rotating frame, and differential orbital elements, allows the characterization of small orbital element differences in terms of the constants of the HCW solutions, viz. relative orbit size and phase. This feature has been used by Refs. [25, 26] to design formations in near-circular orbits. The basic zero-secular drift condition is satisfied by setting the semi-major axis of the Deputy and Chief to be the same. The characterization of relative orbit geometry is achieved by relating the rest of the orbital element differences to its shape, size, and the initial phase angle.

Even though relative motion near an arbitrary Keplerian elliptic orbit is well-represented in the literature, the characterization of formations in such orbits has still not been addressed completely. Schaub[27] related the differential orbital elements to the constants of the HCW solution for near-circular references orbits. Lane and Axelrad[28] expressed relative motion near elliptic orbits, in terms of integration constants and differential orbital elements. Zanon and Campbell[29] discussed the effects of the constants of integration in the solution to the Tschauner-Hempel equations, on the relative motion equations. The last two works are useful for mission design near arbitrarily eccentric orbits; however, some key issues still require exploration, for example, how the choice of the constants or orbit eccentricity affect the relative orbit shape and size.

This paper presents a meaningful parameterization for formation geometry, near elliptic orbits of arbitrarily eccentricity, in terms of parameters which are analogous to the special case of the HCW constants. These parameters are directly related to orbit shape and size, unlike previous works, in the sense that they provide useful and direct insight into the relative orbit geometry, for arbitrarily eccentric orbits. These parameters are derived using the Tschauner-Hempel (TH) model as a basis. This model is useful in deriving a simple linear relationship between the initial conditions that lead to bounded motion, for arbitrary

eccentricity and epoch. By simple manipulation, the unity between the TH model and the geometric method as proposed by Alfriend *et al.*[25] is revealed, and the linear relationships between the new parameterization, constants of integration of the TH model, and differential orbital elements, are developed. Furthermore, by the use of Fourier-Bessel expansions using the true and mean anomalies as independent variables, the effects of eccentricity on formation geometry are characterized. The use of the new parameterization intuitively reveals these effects, and schemes for formation design are suggested that accomodate eccentricity effects. Both, true anomaly, as well as time, are treated as the independent variable in this approach.

General Solution to TH Relative Motion Equations

Consider an Earth-centered inertial (ECI) frame, denoted by $\mathcal{N}$, with orthonormal basis $\mathcal{B}_N = \{\mathbf{i}_x \quad \mathbf{i}_y \quad \mathbf{i}_z\}$. The vectors $\mathbf{i}_x$ and $\mathbf{i}_y$ lie in the equatorial plane, with $\mathbf{i}_x$ coinciding with the line of the equinoxes, and $\mathbf{i}_z$ passes through the North Pole. The analysis uses a Local-Vertical-Local-Horizontal (LVLH) frame, as shown in Fig. 1 and denoted by $\mathcal{L}$, that is attached to the target satellite (also called Leader or Chief). This frame has basis $\mathcal{B}_L = \{\mathbf{i}_r \quad \mathbf{i}_\theta \quad \mathbf{i}_h\}$, with $\mathbf{i}_r$ lying along the radius vector from the Earth's center to the satellite, $\mathbf{i}_h$ coinciding with the normal to the plane defined by the position and velocity vectors of the satellite, and $\mathbf{i}_\theta = \mathbf{i}_h \times \mathbf{i}_r$. The TH equations[20] use the true anomaly of the Chief, f as the independent variable, instead of time, t. Let the position of the Deputy in the Chief's LVLH frame be denoted by $\boldsymbol{\varrho} = u\mathbf{i}_r + v\mathbf{i}_\theta + w\mathbf{i}_h$, where u, v and w denote the components of the position vector along the radial, along-track, and out-of-plane directions, respectively. The position is normalized with respect to the radius of the Chief, $r = p/(1 + e\cos f)$, where $p = a\eta^2$ is the semiparameter, a is the semimajor axis, $\eta = \sqrt{(1 - e^2)}$, and e is the eccentricity. The normalized position vector is given as follows:

$$\boldsymbol{\rho} = x\mathbf{i}_r + y\mathbf{i}_\theta + z\mathbf{i}_h = (1 + e\cos f)\frac{\boldsymbol{\varrho}}{p} \tag{1a}$$

$$\boldsymbol{\rho}' = (1 + e\cos f)\frac{\boldsymbol{\varrho}'}{p} - e\sin f\frac{\boldsymbol{\varrho}}{p} \tag{1b}$$

$$\boldsymbol{\rho}'' = (1 + e\cos f)\frac{\boldsymbol{\varrho}''}{p} - 2e\sin f\frac{\boldsymbol{\varrho}'}{p} - e\cos f\frac{\boldsymbol{\varrho}}{p} \tag{1c}$$

where x, y, and z are the components of the normalized relative position, and $(')$ and $('')$ denote derivatives with respect to f. The relative motion equations using the normalized position and velocity (TH equations) are:

$$x'' - 2y' - \frac{3x}{(1 + e\cos f)} = 0 \tag{2a}$$

$$y'' + 2x' = 0 \tag{2b}$$

$$z'' + z = 0 \tag{2c}$$

Equations (2) have the following general solution[30, 31]:

$$x(f) = \frac{d_1}{e}\cos f\,(1 + e\cos f) + d_2 \sin f\,(1 + e\cos f) + d_3 \sin f\,(1 + e\cos f) I(f) \tag{3a}$$

$$y(f) = -\frac{d_1}{e}\sin f\,(2 + e\cos f) + \frac{d_2}{e}\,(1 + e\cos f)^2 + \frac{d_3}{e}\left[(1 + e\cos\theta)^2 I(f) + \cot f\right] + d_4 \tag{3b}$$

$$z(f) = d_5 \cos f + d_6 \sin f \tag{3c}$$

where

$$I(f) = \int_{f_0}^{f} \frac{1}{\sin^2 f\,(1 + e\cos f)^2}\,df \tag{4}$$

As shown in Ref. [31], Eq. (4) is easily evaluated in terms of the eccentric anomaly, E, which is related to the true anomaly by the following equation:

$$\tan\frac{f}{2} = \sqrt{\frac{1+e}{1-e}}\tan\frac{E}{2} \tag{5}$$

However, $I(f)$ has a singularity for $f = n\pi$, which can be removed, as shown by Carter[32], by integrating Eq. (4) by parts:

$$I(f) = 2e\int_{f_0}^{f} \frac{\cos f}{(1 + e\cos f)^3}\,df - \frac{\cot f}{(1 + e\cos f)^2} + c_J = 2e\,J(f) - \frac{\cot f}{(1 + e\cos f)^2} + c_J \tag{6}$$

where c_J is an arbitrary constant. Carter[33] has shown that the state transition matrix formulated utilizing $J(f)$ also has singularities when $e = 0$, which can be removed if $J(f)$ too, is integrated by parts. Yamanaka and Ankersen[19] have shown that $J(f)$ may also be conveniently rewritten in terms of Kepler's equation[23], to be uniformly valid for $0 \leq e < 1$. As will be shown later, this step also demonstrates the unity between the TH solutions and the differential orbital element approach[25], by revealing a linear relationship between the constants of integration of the former approach, and differential orbital elements of the latter approach. The integral $J(f)$ is rewritten as:

$$J(f) = -\frac{3e}{2\eta^5}K(f) + \frac{1}{2\eta^2}\frac{\sin f\,(2 + e\cos f)}{(1 + e\cos f)^2} \tag{7}$$

$$\text{where,} \qquad K(f) = \int_{f_0}^{f} \frac{\eta^3}{(1 + e\cos f)^2}\,df = (E - e\sin E) - (E_0 - e\sin E_0) = n\,\Delta t \tag{8}$$

where $n = \sqrt{(\mu/a^3)}$ is the mean motion of the reference orbit, and Δt is the elapsed time since epoch. The constants are rearranged for convenience in the following fashion: $c_1 = d_1/e - d_3/\eta^2$, $c_2 = d_2 + d_3 c_J$, $c_3 = e d_3$, $c_4 = d_2/e + d_3 c_J/e + d_4$, and $c_{5,6} = d_{5,6}$. Then, the solutions to the TH equations are:

$$x(f) = c_1 \cos f\,(1 + e\cos f) + c_2 \sin f\,(1 + e\cos f) + \frac{2c_3}{\eta^2}\left[1 - \frac{3e}{2\eta^3}\sin f\,(1 + e\cos f)K(f)\right] \tag{9a}$$

$$y(f) = -c_1 \sin f\,(2 + e\cos f) + c_2 \cos f\,(2 + e\cos f) - \frac{3c_3}{\eta^5}(1 + e\cos f)^2 K(f) + c_4 \tag{9b}$$

$$z(f) = c_5 \cos f + c_6 \sin f \tag{9c}$$

The relative velocity components are as follows:

$$\begin{aligned} x'(f) &= -c_1(\sin f + e\sin 2f) + c_2(\cos f + e\cos 2f) \\ &\quad -\frac{3ec_3}{\eta^2}\left[\frac{\sin f}{(1 + e\cos f)} + \frac{1}{\eta^3}(\cos f + e\cos 2f)K(f)\right] \end{aligned} \tag{10a}$$

$$\begin{aligned} y'(f) &= -c_1(2\cos f + e\cos 2f) - c_2(2\sin f + e\sin 2f) \\ &\quad -\frac{3c_3}{\eta^2}\left[1 - \frac{e}{\eta^3}(2\sin f + e\sin 2f)K(f)\right] \end{aligned} \tag{10b}$$

$$z'(f) = -c_5 \sin f + c_6 \cos f \tag{10c}$$

The constants of integration can be evaluated in terms of the initial conditions, and are related to the pseudoinitial values used in Ref. [19]. Let the initial conditions be denoted by $\mathbf{x}_0 = \{x_0\ y_0\ z_0\ x_0'\ y_0'\ z_0'\}^\top$, specified at arbitrary initial true anomaly f_0, and let the vector of integration constants be denoted by $\mathbf{c} = \{c_1 \cdots c_6\}^\top$. Then, $\mathbf{x}_0 = \mathbf{L}(f_0)\mathbf{c}$ where the (i,j)th entry of $\mathbf{L}$ is the term with c_j as a coefficient, in the expression for the ith component of the state vector. It can be shown that $\det \mathbf{L} = 1$, and if $\mathbf{M}$ denotes the inverse of $\mathbf{L}$, then $\mathbf{M} = \text{adjoint}\,\mathbf{L}$. It follows that $\mathbf{c} = \mathbf{M}(f_0)\mathbf{x}_0$, where:

$$\begin{aligned} c_1 &= -\frac{3}{\eta^2}(e + \cos f_0)x_0 - \frac{1}{\eta^2}\sin f_0\,(1 + e\cos f_0)x_0' \\ &\quad -\frac{1}{\eta^2}(2\cos f_0 + e + e\cos^2 f_0)y_0' \end{aligned} \tag{11a}$$

$$c_2 = -\frac{3}{\eta^2}\frac{\sin f_0(1 + e\cos f_0 + e^2)}{(1 + e\cos f_0)}x_0 + \frac{1}{\eta^2}(\cos f_0 - 2e + e\cos^2 f_0)x_0'$$

$$-\frac{1}{\eta^2}\sin f_0(2+e\cos f_0)y_0' \tag{11b}$$

$$c_3 = (2+3e\cos f_0+e^2)\,x_0 + e\sin f_0\,(1+e\cos f_0)\,x_0' + (1+e\cos f_0)^2\,y_0' \tag{11c}$$

$$c_4 = -\frac{1}{\eta^2}(2+e\cos f_0)\left[\frac{3e\sin f_0}{(1+e\cos f_0)}x_0 + (1-e\cos f_0)x_0' + e\sin f_0 y_0'\right] + y_0 \tag{11d}$$

$$c_5 = \cos f_0\, z_0 - \sin f_0\, z_0' \tag{11e}$$

$$c_6 = \sin f_0\, z_0 + \cos f_0\, z_0' \tag{11f}$$

Since $\mathbf{x}(f) = \mathbf{L}(f)\mathbf{c} = \mathbf{L}(f)\mathbf{M}(f_0)\mathbf{x}_0$, the state transition matrix[19] for this system is $\mathbf{\Phi}(f, f_0) = \mathbf{L}(f)\mathbf{M}(f_0)$.

Mapping Between States and Differential Orbital Elements

In the geometric description for relative motion, the position in the LVLH frame is written in terms of differential orbital elements by linearizing the direction cosine matrix that orients the Deputy LVLH frame with respect to the Chief LVLH frame. Alfriend *et al.*[25] have shown that:

$$u = \delta r \tag{12a}$$

$$v = r(\delta\theta + \delta\Omega\cos i) \tag{12b}$$

$$w = r(\delta i\sin\theta - \delta\Omega\sin i\cos\theta) \tag{12c}$$

where δœ denotes a small change in the orbital element œ. Dividing by r to get the corresponding normalized states,

$$x = \delta r/r \tag{13a}$$

$$y = \delta\theta + \delta\Omega\cos i \tag{13b}$$

$$z = \delta i\sin\theta - \delta\Omega\sin i\cos\theta \tag{13c}$$

Following the development in Ref. [27], it can be shown that:

$$\frac{\delta r}{r} = \frac{e}{\eta^3}\sin f(1+e\cos f)\delta M_0 - \frac{1}{\eta^2}\cos f(1+e\cos f)\delta e + \left[1 - \frac{3e}{2\eta^3}\sin f\,(1+e\cos f)\,n\,\Delta t\right]\frac{\delta a}{a} \tag{14}$$

wherein the fact that the mean anomaly difference, δM is the sum of its initial value, δM_0, and the difference in mean motion propagated over the elapsed time since epoch, has been

used:

$$\delta M = \delta M_0 + \delta n\, \Delta t = \delta M_0 - \frac{3}{2} n\, \Delta t\, \frac{\delta a}{a} \tag{15}$$

Since from Eq. (8), $n\,\Delta t = K(f)$, a direct correspondence between Eq. (14) and Eq. (9*a*) is observed:

$$\delta a = \frac{2a}{\eta^2} c_3 \tag{16}$$

$$\delta M_0 = \frac{\eta^3}{e} c_2 \tag{17}$$

$$\delta e = -\eta^2 c_1 \tag{18}$$

Comparing the expression for z from Eqs. (13) with Eq. (9*c*), the following are obtained:

$$\delta i \sin\omega - \delta\Omega \sin i \cos\omega = c_5 \tag{19a}$$

$$\delta i \cos\omega + \delta\Omega \sin i \sin\omega = c_6 \tag{19b}$$

Consequently,

$$\delta i = \sin\omega\, c_5 + \cos\omega\, c_6 = \sin\theta_0\, z_0 + \cos\theta_0\, z_0' \tag{20}$$

$$\delta\Omega \sin i = -\cos\omega\, c_5 + \sin\omega\, c_6 = -(\cos\theta_0\, z_0 - \sin\theta_0\, z_0') \tag{21}$$

where $\theta_0 = \omega + f_0$. Finally, comparing the expression for y from Eqs. (13) with Eq. (9*b*), the following result is obtained:

$$\delta\omega = c_4 - \frac{\delta M_0}{\eta^3} - \delta\Omega \cos i \tag{22}$$

Thus, the orbital element differences (to the first order) can be obtained by substituting $c_{1\ldots6}$ in the above equations. Let $\boldsymbol{\delta oe} = \{\delta a\ \delta e\ \delta i\ \delta\Omega\ \delta\omega\ \delta M_0\}^\top$ denote the vector of differential orbital elements. Let $\mathbf{oe}_C$ denote the orbital elements of the Chief. Then the equations relating differential orbital elements to the constants of integration as shown above, may be summarized by $\boldsymbol{\delta oe} = \mathbf{N}(\mathbf{oe}_C)\mathbf{c}$, where the matrix $\mathbf{N}$ has as its entries, the coefficients of the integration constants comprising the differential orbital elements. Consequently, the relation $\boldsymbol{\delta oe} = \mathbf{N}(\mathbf{oe}_C)\mathbf{M}(f_0)\mathbf{x}_0$ yields the differential orbital elements in terms of the initial conditions. It can be shown that $\det\mathbf{N} = 2\eta^3 a/(e\sin i)$ and $\det\mathbf{M} = 1$; this means the mapping from relative Cartesian coordinates to differential orbital elements is singular when the reference orbit is circular or equatorial ($e = 0$ or $i = 0$, respectively). In particular, if e

is a small number (or zero), then calculations for δM_0 and $\delta\omega$ from Eq. (17) and Eq. (22), respectively, yield large numbers (or are undefined) due to e appearing in the denominator. However, their sum is a small number, consistent with assumption of small orbital element differences. This problem may be solved by using nonsingular orbital elements[23]. The solutions to the TH equations, and the development of differential nonsingular orbital elements in terms of the initial conditions are presented in the appendix. The singularity due to $e = 0$ also ceases to be a problem if the parameterization developed in this paper, is used. However, for the following sections, results are shown using the classical orbital element set since they are more concisely expressed in terms of these elements.

Drift due to Mismatched Semimajor Axes

If δa (and consequently, c_3) is not zero, then from Eqs. (9) it is evident that x and y will grow in an unbounded fashion, due to the presence of $K(f)$, which is an increasing function. After one orbit of the Chief, the drift in x and y directions are thus:

$$x_{\text{drift}} = x(f_0 + 2\pi) - x(f_0) = -\frac{6\pi c_3}{\eta^5} e \sin f_0 \,(1 + e\cos f_0) \tag{23a}$$

$$y_{\text{drift}} = y(f_0 + 2\pi) - y(f_0) = -\frac{6\pi c_3}{\eta^5} (1 + e\cos f_0)^2 \tag{23b}$$

The drift in unscaled coordinates, in terms of differential semimajor axis, can be calculated to yield the following:

$$u_{\text{drift}} = -\frac{3\pi}{\eta}\, e \sin f_0 \,\delta a \tag{24a}$$

$$v_{\text{drift}} = -\frac{3\pi}{\eta}\, (1 + e\cos f_0)\,\delta a \tag{24b}$$

Thus the total drift in position per orbit, denoted by $\varrho_{\text{drift}}/\text{orbit}$ is:

$$\varrho_{\text{drift}}/\text{orbit} = \left(u_{\text{drift}}^2 + v_{\text{drift}}^2\right)^{1/2} = \frac{3\pi}{\eta}\,\delta a\,(1 + e^2 + 2e\cos f_0)^{1/2} \tag{25}$$

This drift is maximum at $f_0 = 0$, and minimum at $f_0 = \pi$, and is bounded as shown below:

$$3\pi\,\delta a\sqrt{\frac{1-e}{1+e}} \le \varrho_{\text{drift}}/\text{orbit} \le 3\pi\,\delta a\sqrt{\frac{1+e}{1-e}} \tag{26}$$

The maximum and minimum value of the drift were also obtained by Carpenter and Alfriend[34] by evaluating the relative drift and apoapsis and periapsis only.

Periodic Orbits

Periodic solutions may be obtained by choosing initial conditions such that $c_3 = 0$, since the rest of the terms in the solution are sinusoids, and therefore, periodic. Consequently, Eq. (11c) results in the following relation for bounded relative motion:

$$(2 + 3e\cos f_0 + e^2)\, x_0 + e\sin f_0\,(1 + e\cos f_0)\, x_0' + (1 + e\cos f_0)^2\, y_0' = 0 \tag{27}$$

In unscaled coordinates, this is transformed into the following linear condition for bounded relative motion, for arbitrary eccentricity and epoch:

$$\begin{aligned}&(2 + e\cos f_0)\,(1 + e\cos f_0)^2 \left(\frac{u}{p}\right) + e\sin f_0 \left(\dot{u}\sqrt{\frac{p}{\mu}}\right)\\ &-e\sin f_0\,(1 + e\cos f_0)^2 \left(\frac{v}{p}\right) + (1 + e\cos f_0) \left(\dot{v}\sqrt{\frac{p}{\mu}}\right) = 0\end{aligned} \tag{28}$$

In the above equation, the symbol $(\dot{})$ is used to signify a derivative with respect to time; consequently, $\dot{u}$ and $\dot{v}$ are radial and along-track components of the dimensional velocities in the rotating frame of the Chief.

Equation (27) is satisfied for an infinite combination of initial conditions, except when $f_0 = 0$ or $f_0 = \pi$. Furthermore, when $e = 0$, this reduces to the well-known Hill's condition for periodicity. Without loss of generality, one may choose:

$$y_0' = -\frac{(2 + 3e\cos f_0 + e^2)}{(1 + e\cos f_0)^2} x_0 - \frac{e\sin f_0}{(1 + e\cos f_0)} x_0' \tag{29}$$

With $c_3 = 0$, the expressions for the trajectory are considerably simplified. Upon substituting Eq. (29) in Eqs. (11), the constants may be rewritten in terms of dimensional position and velocity with f as the independent variable,

$$c_1 = \frac{(\cos f_0 + e\cos 2f_0)}{(1 + e\cos f_0)^2} x_0 - \frac{\sin f_0}{(1 + e\cos f_0)} x_0' = \frac{u_0}{p}\cos f_0 - \frac{u_0'}{p}\sin f_0 \tag{30a}$$

$$c_2 = \frac{(\sin f_0 + e\sin 2f_0)}{(1 + e\cos f_0)^2} x_0 + \frac{\cos f_0}{(1 + e\cos f_0)} x_0' = \frac{u_0}{p}\sin f_0 + \frac{u_0'}{p}\cos f_0 \tag{30b}$$

$$c_4 = y_0 - \frac{(2 + e\cos f_0)}{(1 + e\cos f_0)} \left(\frac{e\sin f_0}{1 + e\cos f_0} x_0 + x_0'\right) = \frac{v_0}{p}(1 + e\cos f_0) - \frac{u_0'}{p}(2 + e\cos f_0) \tag{30c}$$

$$c_5 = z_0\cos f_0 - z_0'\sin f_0 = \frac{w_0}{p}(\cos f_0 + e) - \frac{w_0'}{p}\sin f_0(1 + e\cos f_0) \tag{30d}$$

$$c_6 = z_0\sin f_0 + z_0'\cos f_0 = \frac{w_0}{p}\sin f_0 + \frac{w_0'}{p}\cos f_0(1 + e\cos f_0) \tag{30e}$$

A concise representation of the most general solution for periodic motion near a Keplerian elliptic orbit with linearized differential gravity, denoted by the subscript '$\wp$', is given by:

$$x_\wp(f) = \frac{\varrho_1}{p}\sin(f+\alpha_0)\,(1+e\cos f) \tag{31a}$$

$$y_\wp(f) = \frac{\varrho_1}{p}\cos(f+\alpha_0)\,(2+e\cos f) + \frac{\varrho_2}{p} \tag{31b}$$

$$z_\wp(f) = \frac{\varrho_3}{p}\sin(f+\beta_0) \tag{31c}$$

where the new relative orbit parameters, $\varrho_{1\ldots3}$, α_0, and β_0, are obtained from Eqs. (30), and are given by:

$$\varrho_1 = \left(u_0^2 + u_0'^2\right)^{1/2} = \frac{a}{\eta}\left(\eta^2\delta e^2 + e^2\delta M_0^2\right)^{1/2} \tag{32a}$$

$$\varrho_2 = v_0(1+e\cos f_0) - u_0'(2+e\cos f_0) = p\left(\delta\omega + \delta\Omega\cos i + \frac{1}{\eta^3}\delta M_0\right) \tag{32b}$$

$$\begin{aligned}\varrho_3 &= \left[(1+2e\cos f_0+e^2)w_0^2 + (1+e\cos f_0)^2 w_0'^2 - 2e\sin f\,(1+e\cos f)w_0w_0'\right]^{1/2} \\ &= p\left(\delta i^2 + \delta\Omega^2\sin^2 i\right)^{1/2}\end{aligned} \tag{32c}$$

$$\alpha_0 = \tan^{-1}\left(\frac{u_0}{u_0'}\right) - f_0 = \tan^{-1}\left(-\frac{\eta}{e}\frac{\delta e}{\delta M_0}\right) \tag{32d}$$

$$\beta_0 = \tan^{-1}\left(\frac{(1+e\cos f_0)w_0}{(1+e\cos f_0)w_0' - e\sin f_0 w_0}\right) - f_0 = \tan^{-1}\left(-\frac{\delta\Omega\sin i}{\delta i}\right) + \omega \tag{32e}$$

The constants $c_{1\ldots6}$ may be expressed using the design parameters, as shown:

$$c_1 = \frac{\varrho_1}{p}\sin\alpha_0, \quad c_2 = \frac{\varrho_1}{p}\cos\alpha_0, \quad c_4 = \frac{\varrho_2}{p}, \quad c_5 = \frac{\varrho_3}{p}\sin\beta_0, \quad c_6 = \frac{\varrho_3}{p}\cos\beta_0 \tag{33}$$

Obviously, the most general form of periodic solutions to the HCW equations are a special case of Eqs. (31).

Two advantages of using the new parameterization have been mentioned earlier, viz. their uniform validity for all eccentricities, and the fact that ϱ_1 and ϱ_3 are obviously size parameters, ϱ_2 is a bias parameter, and α_0 and β_0 are phase angle parameters. Therefore, the effects of the changing one or more of these parameters is intuitively clear. Furthermore, the concise nature of this parameterization proves very useful for the study of more complicated models of relative motion, as shown by Sengupta *et al.*[14].

The differential orbital elements may also be rewritten in terms of the parameter set. These relations are useful, for example, if Gauss' variational equations are used to initiate a numerical procedure for formation establishment or reconfiguration. Such an approach was used by Vaddi *et al.*[35], to establish and reconfigure formations near circular orbits, using

impulsive thrust. Upon substituting Eq. (33) into Eqs. (16)-(22), and setting $c_3 = 0$, results in the following:

$$\delta a = 0 \tag{34a}$$

$$\delta e = -\eta^2 c_1 = -\frac{\varrho_1}{a}\sin\alpha_0 \tag{34b}$$

$$\delta i = \sin\omega\, c_5 + \cos\omega\, c_6 = \frac{\varrho_3}{p}\cos(\beta_0 - \omega) \tag{34c}$$

$$\delta\Omega = \frac{1}{\sin i}\left(-\cos\omega\, c_5 + \sin\omega\, c_6\right) = -\frac{\varrho_3}{p}\frac{\sin(\beta_0 - \omega)}{\sin i} \tag{34d}$$

$$\delta M_0 = \frac{\eta^3}{e}c_2 = \frac{\varrho_1}{a}\frac{\eta}{e}\cos\alpha_0 \tag{34e}$$

$$\delta\omega = \frac{\varrho_2}{p} - \frac{\delta M_0}{\eta^3} - \delta\Omega\cos i \tag{34f}$$

Corresponding expressions for nonsingular orbital elements are presented in the appendix.

Eccentricity-Induced Effects on Orbit Geometry

The most general form of periodic motion in the setting of the HCW equations is given by the following equations (wherein subscript 'h' denotes HCW solutions):

$$u_h = k_1\sin(\tau + \varphi_0) \tag{35a}$$

$$v_h = 2k_1\cos(\tau + \varphi_0) + k_2 \tag{35b}$$

$$w_h = k_3\sin(\tau + \psi_0) \tag{35c}$$

where $\tau = nt$ is the normalized time or mean anomaly, though in the case of the HCW equations, this is equivalent to true anomaly since eccentricity is assumed zero. The actual relative orbit has a trajectory in the local frame whose components are given by the following expressions:

$$u_\wp = rx_\wp = \varrho_1\sin(f + \alpha_0) \tag{36a}$$

$$v_\wp = ry_\wp = 2\varrho_1\cos(f + \alpha_0)\frac{(1 + (e/2)\cos f)}{(1 + e\cos f)} + \frac{\varrho_2}{(1 + e\cos f)} \tag{36b}$$

$$w_\wp = rz_\wp = \varrho_3\frac{\sin(f + \beta_0)}{(1 + e\cos f)} \tag{36c}$$

Eccentricity effects may be studied by expanding $v_\wp$ and $w_\wp$ as Fourier series. In this section, the effects of eccentricity are analyzed by using both true anomaly, and time as the independent variable.

True Anomaly as the Independent Variable

The Cauchy residue theorem is now used to obtain the coefficients of $\cos kf$ and $\sin kf$ to form Fourier series for $v_\wp$ and $w_\wp$. This is similar to the approach used in Ref. [23] to obtain a series expansion of eccentric anomaly in terms of mean anomaly. It can be shown that:

$$\cos f\,\frac{(2+e\cos f)}{(1+e\cos f)} = -\frac{\varepsilon}{\eta} + \frac{(2+\eta+\eta^2)}{\eta(1+\eta)}\cos f + \frac{2}{\eta(1+\eta)}\sum_{k=2}^{\infty}(-\varepsilon)^{k-1}\cos kf \quad (37a)$$

$$\sin f\,\frac{(2+e\cos f)}{(1+e\cos f)} = \frac{(3+\eta)}{(1+\eta)}\sin f + \frac{2}{(1+\eta)}\sum_{k=2}^{\infty}(-\varepsilon)^{k-1}\sin kf \quad (37b)$$

$$\frac{1}{(1+e\cos f)} = \frac{1}{\eta} + \frac{2}{\eta}\sum_{k=1}^{\infty}(-\varepsilon)^{k}\cos kf \quad (37c)$$

where $\varepsilon = \sqrt{[(1-\eta)/(1+\eta)]} = \mathcal{O}(e)$. Consequently,

$$\begin{aligned} v_\wp(f) &= \left[-\frac{\varepsilon}{\eta}\varrho_1\cos\alpha_0 + \frac{1}{\eta}\varrho_2\right] \quad (38a)\\ &+ \left[\frac{(2+\eta+\eta^2)}{\eta(1+\eta)}\varrho_1\cos\alpha_0 - 2\frac{\varepsilon}{\eta}\varrho_2\right]\cos f - \frac{(3+\eta)}{(1+\eta)}\varrho_1\sin\alpha_0\sin f\\ &+\frac{2}{\eta(1+\eta)}\sum_{k=2}^{\infty}(-\varepsilon)^{k-1}\Big[\{\varrho_1\cos\alpha_0 - \varepsilon(1+\eta)\varrho_2\}\cos kf - \eta\varrho_1\sin\alpha_0\,\sin kf\Big]\\ w_\wp(f) &= -\frac{\varepsilon}{\eta}\varrho_3\sin\beta_0 + \frac{2}{\eta(1+\eta)}\varrho_3\,(\eta\cos\beta_0\,\sin f + \sin\beta_0\,\cos f) \quad (38b)\\ &+\frac{2}{\eta(1+\eta)}\varrho_3\sum_{k=2}^{\infty}(-\varepsilon)^{k-1}\,(\eta\cos\beta_0\,\sin kf + \sin\beta_0\,\cos kf) \end{aligned}$$

It is observed that both the v and w components of motion have constant terms, a primary harmonic, associated with relative orbit size parameters, and higher-order harmonics. Thus the five effects of eccentricity are immediately recognized. The first effect is obviously the presence of higher-order harmonics, whose amplitudes successively decrease by a factor of ε. For non-zero eccentricities, this causes deviation from the well-known circular shape of the HCW solutions.

The second effect is that of amplitude scaling, as may be observed by the presence of terms dependent on η in the amplitudes of the primary harmonics in both v and w. Consequently, as eccentricity increases, for the same choice of $\varrho_{1\ldots3}$, the orbit tends to shrink in the along-track direction and expand in the out-of-plane direction.

The third effect of eccentricity is the introduction of a phase shift. This is readily observed

by recasting Eq. (38*b*) as:

$$w_\wp(f) = -\frac{\varepsilon}{\eta}\varrho_3 \sin\beta_0 + \frac{2}{\eta(1+\eta)}\left(\sin^2\beta_0 + \eta^2\cos^2\beta_0\right)^{1/2}\varrho_3 \sin\left(f+\widetilde{\beta}_0\right) \tag{39}$$
$$+\frac{2}{\eta(1+\eta)}\left(\sin^2\beta_0 + \eta^2\cos^2\beta_0\right)^{1/2}\varrho_3 \sum_{k=2}^{\infty}(-\varepsilon)^{k-1}\sin\left(kf+\widetilde{\beta}_0\right)$$

where

$$\widetilde{\beta}_0 = \tan^{-1}\left(\frac{1}{\eta}\tan\beta_0\right) = \beta_0 + \frac{e^2}{4}\sin 2\beta_0 + \frac{e^4}{8}\left(\sin 2\beta_0 + \frac{1}{4}\sin 4\beta_0\right) + \mathcal{O}(e^6) \tag{40}$$

Furthermore, the phase angle of the Deputy also affects its amplitude.

A fourth effect renders the formation off-center, due to the presence of constant terms in the $v_\wp$ and $w_\wp$ components of motion. The bias depends on the phase angles α_0 and β_0 of the Deputy. While the bias in $w_\wp$ cannot be controlled since ϱ_3 is specified by relative orbit design requirements, the bias in $v_\wp$ can be removed by an appropriate choice of ϱ_2.

The appearance of higher-order harmonics in $v_\wp$ and $w_\wp$, but not in $u_\wp$, causes the fifth effect - that of skewness of the relative orbit plane. When formations require the phase angles in the along-track and out-of-plane to be equal, the radial motion is in-phase with the along-track, and consequently, out-of-plane motion. Consequently, a plot of the out-of-plane motion vs. the radial motion would result in a straight line. However, due to eccentricity effects, higher-order harmonics appear in $w_\wp$, but not in $u_\wp$. The relative orbit is therefore no longer planar. This will be demonstrated in the context of Projected Circular Orbit solutions.

The bias and skewness of the relative orbit are well-known, as reported by Refs. [16, 29]. The bias, and the other three effects, can be corrected to some extent by appropriate initial conditions. However, it is necessary to analyze these effects with time, which is the independent variable enforced by physics.

Time as the Independent Variable

If the normalized time τ is chosen as the independent variable, then the relative motion expressions are qualitatively the same, i.e., they exhibit the same properties as in the previous section. However, in the quantitative sense, the equations are different. In this section use is made of the following relations[23]:

$$\cos kM = \sum_{n=-\infty}^{\infty} J_n(-ke)\cos(n+k)E \tag{41a}$$

$$\sin kM = \sum_{n=-\infty}^{\infty} J_n(-ke)\sin(n+k)E \tag{41b}$$

where J_n are Bessel functions of the first kind of order n, and

$$J_n(\nu) = \sum_{l=0}^{\infty} \frac{(-1)^l}{2^{2l+n}\, l!\,(n+l)!}\nu^{2l+n} \tag{42}$$

It can then be shown that:

$$v_{\wp}(\tau) = (a_0\varrho_1\cos\alpha_0 + c_0\varrho_2) + \sum_{k=1}^{\infty}\Big[\,(a_k\varrho_1\cos\alpha_0 + c_k\varrho_2)\cos k\tau - b_k\sin\alpha_0\sin k\tau\Big] \tag{43a}$$

$$w_{\wp}(\tau) = p_0\varrho_3\sin\beta_0 + \varrho_3\sum_{k=1}^{\infty}(p_k\sin\beta_0\cos k\tau + q_k\cos\beta_0\sin k\tau) \tag{43b}$$

where,

$$a_0 = -\frac{e}{2\eta^2}(3+2\eta^2), \quad a_k = -\frac{(1-k\eta^4)}{k\eta^2}J_{k+1}(ke) + \frac{(1+k\eta^4)}{k\eta^2}J_{k-1}(ke) \tag{44a}$$

$$b_k = \frac{2}{\eta}\frac{J_k(ke)}{ke} - \eta\,[J_{k+1}(ke) - J_{k-1}(ke)] \tag{44b}$$

$$c_0 = \frac{3-\eta^2}{2\eta^2}, \quad c_k = \frac{e}{k\eta^2}\,[J_{k+1}(ke) - J_{k-1}(ke)] \tag{44c}$$

$$p_0 = -\frac{3e}{2\eta^2}, \quad p_k = -\frac{1}{k\eta^2}\,[J_{k+1}(ke) - J_{k-1}(ke)] \tag{44d}$$

$$q_k = \frac{2}{\eta}\frac{J_k(ke)}{ke} \tag{44e}$$

Even though b_k and q_k have e in the denominator, the computation of these expressions do not cause problems as $e \to 0$, because of the following expansion:

$$\frac{J_k(ke)}{ke} = \sum_{l=0}^{\infty}\frac{(-1)^l}{2^{2l+k}\, l!\,(k+l)!}\,(ke)^{2l+k-1}, \quad k \geq 1 \tag{45}$$

The expansion of $u_{\wp}$ in terms of harmonics of the mean anomaly is straightforward since the equations relating $\cos f$ and $\sin f$ to $\cos kM$ and $\sin kM$ are provided in Battin[23]:

$$\begin{aligned} u_{\wp}(\tau) &= \varrho_1\sin\alpha_0\cos f + \varrho_1\cos\alpha_0\sin f \\ &= -e\varrho_1\sin\alpha_0 + \frac{2\eta^2}{e}\varrho_1\sin\alpha_0\sum_{k=1}^{\infty}J_k(ke)\cos kM \end{aligned}$$

$$-\eta\varrho_1 \cos\alpha_0 \sum_{k=1}^{\infty} [J_{k+1}(ke) - J_{k-1}(ke)] \sin kM \tag{46}$$

Consequently, using a numerical procedure, table lookup, or truncation of the series to the desired order of eccentricity, Eqs. (43*a*), (43*b*), and (46) provide time-explicit expressions for bounded relative motion, which can perform as excellent reference trajectories for formation-keeping.

Correcting for Bias

The problem of bias correction is now studied in detail, for the two choices of the independent variable. Since the bias in $w_\wp$ cannot be controlled, only the bias in $v_\wp$ is examined. An examination of Eq. (38*a*) suggests the following choice of ϱ_2, to correct for bias:

$$\varrho_2 = \varepsilon\varrho_1 \cos\alpha_0 \tag{47}$$

Equation (43*a*) suggests the following condition:

$$\varrho_2 = [e(3 + 2\eta^2)/(3 - \eta^2)]\varrho_1 \cos\alpha_0 \tag{48}$$

However, the bias corrections suggested by Eq. (47), and Eq. (48) have different interpretations. Equation (47) does not offer meaningful physical interpretation, in the sense that it is the average of a quantity of a variable that is a nonlinear function of time. In this sense, Equation (48) is physically more significant, since this correction will imply that the Deputy spends equal amounts of time on either side of the Chief in the along-track direction. It is obvious that both biases converge to zero as the Chief's orbit eccentricity decreases, but have vastly different intepretations for high eccentricities.

This point is illustrated by Fig. 2, for a Chief's eccentricity of 0.6. Let $\varrho_1 = 1/2$, $\varrho_3 = 1$ and $\alpha_0 = \beta_0 = 0$. For a circular reference orbit, these correspond to the HCW initial conditions for a projected circular orbit. If $\varrho_2 = \varepsilon\varrho_1 \cos\alpha_0$, then the variation of $v_\wp$ with respect to τ is shown by the dashed line. It is therefore not immediately apparent that this implies the Deputy is on either side of the Chief in the along track direction, for equal portions of the true anomaly. Moreover, the motion is not symmetric with respect to the $\mathbf{i}_h$ vector since $|v_\wp(-\alpha_0)/\varrho_1| < 2\varrho_1$ and $|v_\wp(\pi - \alpha_0)/\varrho_1| > 2\varrho_1$. If $\varrho_2 = [e(3 + 2\eta^2)/(3 - \eta^2)]\varrho_1 \cos\alpha_0$, then, the variation of $v_\wp$ is depicted by the dotted line. This shows values that are greater than $2\varrho_1$ for regions near the Chief's perigee, and less than $2\varrho_1$ for regions near the Chief's apogee. However, the *time-averaged* value is zero. Thus if the mission requires the Deputy to be near the Chief in the along track direction for large periods of time, this bias correction is suitable.

It is also possible to have initial conditions such that $|v_{\wp}(-\alpha_0)| = |v_{\wp}(\pi - \alpha_0)|$. With this correction, it is also noted that motion in the along-track direction is bounded between $\pm 2\varrho_1$. It is easily shown that the correction corresponding to this condition is given by:

$$\varrho_2 = e\varrho_1 \cos\alpha_0 \tag{49}$$

Direct substitution of this condition in Eq. (36), results in $v_{\wp}(-\alpha_0) = 2\varrho_1$ and $v_{\wp}(\pi - \alpha_0) = -2\varrho_1$. The use of this correction results in the solid line in Fig. 2.

Other versions of bias correction exist in the literature. Vaddi *et al.*[12] and Melton[16] employ a correction that is valid for low eccentricities. Inalhan *et al.*[13] describe a process for obtaining initial relative velocity for symmetric motion, by posing the problem as a linear program. However, any of the corrections derived in this section, are valid for arbitrary eccentricity. For example, using Eqs. (32) and Eq. (49), results in the following:

$$v_0 - 2u_0' = \frac{e\sin f_0}{(1 + e\cos f_0)} u_0 \tag{50}$$

Corrections to HCW Initial Conditions

It is of interest to study the deviation induced from the classical HCW solutions due to eccentricity. The different cases are analyzed individually.

Leader-Follower Formation Modified by an Eccentric Reference Orbit

In the Leader-Follower Formation, the Deputy is at a fixed distance from the Chief, along the reference orbit. In the classical HCW environment, this is obtained by setting $k_1 = k_3 = 0$, and $k_2 = d$ in Eqs. (35), where d is the desired separation of the Deputy from the Chief. However, if $\varrho_1 = \varrho_3 = 0$ and $\varrho_2 = d$ in Eqs. (36), then the Deputy-Chief separation varies from $d/(1+e)$ to $d/(1-e)$, with a time-averaged value of $c_0 d$. Consequently, the correct choice for ϱ_2 should be $\varrho_2 = d/c_0 = 2\eta^2 d/(3-\eta^2)$. Irrespective of whether or not the distance is corrected for, care must be taken that a value of ϱ_2 is chosen to ensure that the minimum separation meets design requirements, because as eccentricity increases, the minimum separation decreases.

Projected Circular Orbit Modified by an Eccentric Reference Orbit

Projected Circular Orbits (PCO) are obtained in the HCW equations by setting $2k_1 = k_3 = \varrho$, and $\psi_0 = \varphi_0$ in Eqs. (35). Consequently, $v_h^2 + w_h^2 = \varrho^2$. However, PCOs can never be obtained near an eccentric reference, as is evident from Eqs. (36). It is possible, however, to choose initial conditions such that the relative orbit is as circular as possible, at least to the first harmonic. Assuming that $\varrho_2 = e\varrho_1 \cos\alpha_0$ is chosen as the zero-bias condition, then

$\varrho_1 = \varrho/2$ is sufficient to ensure that maximum and minimum values of $v_\wp(\tau)$ are consistent with HCW conditions. However, the new phase angle for the first harmonic of $v_\wp(\tau)$ is now $\widetilde{\alpha}_0$, where:

$$\tan\widetilde{\alpha}_0 = \frac{b_1}{a_1 + e}\tan\alpha_0 \tag{51}$$

For consistency, it is desired that the first harmonic of $w_\wp(\tau)$ also have the same phase angle as $v_\wp(\tau)$, so that to the first harmonic, a corrected-PCO is obtained. The phase angle of the first harmonic of $w_\wp(\tau)$ is denoted by $\widetilde{\beta}_0$, where:

$$\tan\widetilde{\beta}_0 = \frac{p_1}{q_1}\tan\beta_0 \tag{52}$$

Consequently,

$$\tan\beta_0 = \frac{q_1}{p_1}\tan\widetilde{\beta}_0 = \frac{q_1}{p_1}\tan\widetilde{\alpha}_0 = \frac{q_1 b_1}{p_1(a_1 + e)}\tan\alpha_0 \tag{53}$$

Finally, though out-of-plane bias cannot be controlled, its amplitude can be corrected so that the time average of $w_\wp(\tau)$ is equal to ϱ. Consequently,

$$\varrho_3 = \frac{\varrho}{\left(p_1^2\sin^2\beta_0 + q_1^2\cos^2\beta_0\right)^{1/2}} \tag{54}$$

It is also possible to ensure that maximum $w_\wp(\tau)$ does not exceed ϱ. From Eqs. (36), the extrema of $w_\wp(f)$ occur when $\cos(f+\beta_0) + e\cos\beta_0 = 0$, or when $f = -\beta_0 \pm \cos^{-1}(-e\cos\beta_0)$. Of these, the negative sign corresponds to minimum $w_\wp(f)$ and positive sign to maximum $w_\wp(f)$. Thus if

$$\varrho_3 = \left(-e\sin\beta_0 + \sqrt{1 - e^2\cos^2\beta_0}\right)\varrho \tag{55}$$

then the maximum deviation in the out-of-plane motion will be bounded by $\pm\varrho$. An issue with this approach is that by placing bounds on the maximum out-of-plane motion, its minimum is also naturally reduced, which may bring the Deputy very close to the Chief.

Figure 3 shows examples of a formation initiated with the corrected and uncorrected initial conditions, for a reference orbit with $e = 0.2$ and $e = 0.7$, with $\alpha_0 = 0°$. In these figures, the ideal PCO is shown as a dashed-dotted line. If the Eqs. (35) are used to generate initial conditions for a PCO, then these will result in unbounded motion since Eq. (29) is not satisfied. However, if Eqs. (35) are used to generate initial conditions for all the states excluding v_0', and Eq. (29) is used to generate an initial condition for v_0', the result

will be a relative orbit that is bounded, but without a circular projection. The extent of this deviation is depicted by dashed line. The solid line depicts the result of applying the amplitude correction developed in this section, and the bias correction from Eq. (49). In both cases, bias in the out-of-plane direction is absent, but as shown in Fig. 3(b), bias in along-track direction is significant. The corrections developed in this paper successfully keep along-track motion bounded to the desired value of 1 km. It should also be observed that for high eccentricities, as shown in in Fig. 3(b), projected motion resembles a triangle; this may be exploited for mission design. The bias in the y direction, which is a function of $\cos\alpha_0$, and consequently is maximum when $\alpha_0 = 0°$, is removed entirely, as is shown in Fig. 3(a).

Fig. 4 shows the effects of eccentricity, if $\alpha_0 = 90°$. In this case, bias in the along-track direction is absent, but out-of-plane bias, which is a function of β_0, is maximum. While there is no significant difference upon application of the corrections in Fig. 4(a), the amplitude correction is evident in Fig. 4(b). As eccentricity increases, the Deputy's maximum displacement out of the plane increases to several kilometers. The amplitude correction limits this excursion.

The effect of eccentricity on the three-dimensional character of the relative orbit is shown in Fig. 5. This figure corresponds to initial conditions consistent with Fig. 3, for three values of eccentricity. The solid line shows the out-of-plane vs. radial motion for a circular reference, which will be a straight line, since the phase angles have been chosen to be equal. However, the dashed line, and the dashed-dotted line, which correspond to $e = 0.3$ and $e = 0.8$, respectively, show that the effect of higher-order harmonics causes increasing deviation from the relative orbit plane.

General Circular Orbit Modified by an Eccentric Reference Orbit

The General Circular Orbit (GCO) is obtained in the HCW sense by requiring that $u_h^2 + v_h^2 + w_h^2 = \varrho^2$. Consequently, $k_1 = \varrho/2$, $k_3 = \sqrt{3}\varrho/2$, $k_2 = 0$, and $\psi_0 = \varphi_0$. These conditions lead to a relative orbit that is circular on a plane (local in the rotating frame). For an eccentric reference, the initial conditions need to be modified, since using the HCW initial conditions do not lead to GCOs. The modifications derived in this section only account for the first harmonic in the Fourier-Bessel expansions of Eq. (36).

Upon choosing $\varrho_3 = (\sqrt{3}/2)\,\varrho/\sqrt{(p_1^2\sin^2\beta_0 + q_1^2\cos^2\beta_0)}$, it is evident that $w_\varrho^2(\tau) = (3/4)\,\varrho^2\sin^2(f+\widetilde{\beta}_0)$. Thus, $\varrho_1 = \varrho/2$ remains a valid choice to obtain a GCO-like relative orbit. The phase angles are chosen in the same fashion as those for the PCO. Figures 6(a) and 6(b) show near-GCO formations for a reference orbit with $e = 0.2$, for $\alpha_0 = 0°$ (maximum y-bias), and $\alpha_0 = 90°$ (maximum z-bias), respectively. The legend in the figures is consistent with the previous section, as is the choice of boundedness condition. Furthermore, similar

to the previous section, the corrections are able to eliminate bias in the y direction, but not in the z direction.

Conclusions

This paper studies the effects of eccentricity on the shape and size of relative orbits. Parameters based upon the relative orbit shape and phase angle are developed. It is shown that these parameters are more meaningful than existing works, to study the effects of eccentricity. The key effects are identified as those that lead to amplitude and phase changes, and introduction of bias. Corrective schemes are proposed that exploit the effects of eccentricity, and in some cases, these lead to relative orbits very close or similar to those predicted by the HCW equations. Since the effects of eccentricity are studied both in a qualitative and quantitative fashion, these results can serve as excellent models for future mission design. Furthermore, the approach in this paper yields results that are valid for all values of orbit eccentricity. The approach in this paper unifies the solutions to the Tschauner-Hempel equations, and the relative motion description using differential orbital elements. By using nonsingular elements, the results are shown to be uniformly valid even when the Chief's orbit is circular. The transformation between the relative orbit parameters and differential orbital elements can be used to design impulsive or continuous maneuvers for the establishment of such formations, at low cost, since they include the full effects of eccentricity. The parameterization is also useful for more complicated analysis for formation flight, for example, nonlinear formation flight.

Appendix

The nonsingular orbital element set comprises the elements $\{a\ i\ \Omega\ q_1\ q_2\ \lambda_0\}^\top$ where $q_1 = e\cos\omega$, $q_2 = e\sin\omega$, and $\lambda_0 = \omega + M_0$ (similarly, $F = \omega + E$, and $\theta = \omega + f$), is the mean (similarly, eccentric, and true) argument of latitude. A solution to the TH equations using θ as the independent variable is easily obtained, by observing that Eqs. (9) may be rewritten as:

$$x(\theta) = (\widetilde{c}_1\cos\theta + \widetilde{c}_2\sin\theta)\,\alpha(\theta) + \frac{2c_3}{\eta^2}\left[1 - \frac{3}{2\eta^3}\beta(\theta)\,\alpha(\theta)\,K(\theta)\right] \tag{56a}$$

$$y(\theta) = (-\widetilde{c}_1\sin\theta + \widetilde{c}_2\cos\theta)\,[1+\alpha(\theta)] - \frac{3c_3}{\eta^5}\,\alpha^2(\theta)K(\theta) + c_4 \tag{56b}$$

$$z(\theta) = c_5\cos\theta + c_6\sin\theta \tag{56c}$$

where,

$$\alpha(\theta) = 1 + q_1\cos\theta + q_2\sin\theta = 1 + e\cos f \tag{57a}$$

$$\beta(\theta) = q_1 \sin\theta - q_2 \cos\theta = e \sin f \tag{57b}$$

The arbitrary constants $\widetilde{c}_1$ and $\widetilde{c}_2$ are evaluated as follows:

$$\begin{aligned}
\widetilde{c}_1 &= c_1 \cos\omega - c_2 \sin\omega \\
&= -\frac{3}{\eta^2 \alpha(\theta_0)} \left[q_1(1+\cos^2\theta_0) + q_2 \sin\theta_0 \cos\theta_0 + (2-\eta^2)\cos\theta_0 \right] x_0 \\
&\quad -\frac{1}{\eta^2} \left[q_1 \sin\theta_0 \cos\theta_0 - q_2(1+\cos^2\theta_0) + \sin\theta_0 \right] x_0' \\
&\quad -\frac{1}{\eta^2} \left[q_1(1+\cos^2\theta_0) + q_2 \sin\theta_0 \cos\theta_0 + 2\cos\theta_0 \right] y_0' \qquad (58a) \\
\widetilde{c}_2 &= c_1 \sin\omega + c_2 \cos\omega \\
&= -\frac{3}{\eta^2 \alpha(\theta_0)} \left[q_1 \sin\theta_0 \cos\theta_0 + q_2(1+\sin^2\theta_0) + (2-\eta^2)\sin\theta_0 \right] x_0 \\
&\quad -\frac{1}{\eta^2} \left[q_1(1+\sin^2\theta_0) - q_2 \sin\theta_0 \cos\theta_0 - \cos\theta_0 \right] x_0' \\
&\quad -\frac{1}{\eta^2} \left[q_1 \sin\theta_0 \cos\theta_0 + q_2(1+\sin^2\theta_0) + 2\sin\theta_0 \right] y_0' \qquad (58b)
\end{aligned}$$

The constants c_5 and c_6 are already nonsingular, and c_4 is rewritten as:

$$c_4 = -\frac{1}{\eta^2} \left[1 + \alpha(\theta_0)\right] \left[\frac{3\beta(\theta_0)}{\alpha(\theta_0)} x_0 + (2 - \alpha(\theta_0)) x_0' + \beta(\theta_0) y_0' \right] + y_0 \tag{59}$$

Furthermore, $K(\theta)$ is Kepler's equation rewritten in nonsingular variables:

$$K(\theta) = (F - q_1 \sin F + q_2 \cos F) - (F_0 - q_1 \sin F_0 + q_2 \cos F_0) = \lambda - \lambda_0 \tag{60}$$

The differential nonsingular orbital elements, δq_1, δq_2, and $\delta\lambda_0$ can be written in terms of the initial conditions as shown:

$$\begin{aligned}
\delta q_1 &= \cos\omega\, \delta e - e \sin\omega\, \delta\omega \\
&= (3q_1 + 3\cos\theta_0) x_0 - q_2 y_0 - q_2 \cot i \cos\theta_0\, z_0 + \sin\theta_0 (1 + q_1 \cos\theta_0 + q_2 \sin\theta_0) x_0' \\
&\quad + \{ q_1 + \cos\theta_0 (2 + q_1 \cos\theta_0 + q_2 \sin\theta_0) \}\, y_0' + q_2 \cot i \sin\theta_0\, z_0' \qquad (61a) \\
\delta q_2 &= \sin\omega\, \delta e + e \cos\omega\, \delta\omega \\
&= (3q_2 + 3\cos\theta_0) x_0 + q_1 y_0 + q_1 \cot i \cos\theta_0\, z_0 - \cos\theta_0 (1 + q_1 \cos\theta_0 + q_2 \sin\theta_0) x_0' \\
&\quad + \{ q_2 + \sin\theta_0 (2 + q_1 \cos\theta_0 + q_2 \sin\theta_0) \}\, y_0' - q_1 \cot i \sin\theta_0\, z_0' \qquad (61b) \\
\delta\lambda_0 &= \delta\omega + \delta M_0 \\
&= \cot i\ (\cos\theta_0\, z_0 - \sin\theta_0\, z_0') + \frac{1}{1+\eta} (2 - \eta - \eta^2 + q_1 \cos\theta_0 + q_2 \sin\theta_0) x_0 + y_0
\end{aligned}$$

$$-\frac{1}{1+\eta}\left\{2\eta+2\eta^2+(q_1\cos\theta_0+q_2\sin\theta_0)(1+q_1\cos\theta_0+q_2\sin\theta_0)\right\}x_0'$$
$$+\frac{1}{1+\eta}(q_1\sin\theta_0-q_2\cos\theta_0)(2+q_1\cos\theta_0+q_2\sin\theta_0)y_0 \tag{61c}$$

Equations (61) are free from singularities when $e=0$, but are more complicated than the corresponding expressions for the classical orbital elements.

The most general form for periodic relative motion is also modified, since f cannot be uniquely determined. Therefore, Eqs. (31) are rewritten as:

$$x_{\wp}(f) = \frac{\varrho_1}{p}\sin(\theta+\widetilde{\alpha}_0)\,(1+q_1\cos\theta+q_2\sin\theta) \tag{62a}$$
$$y_{\wp}(f) = \frac{\varrho_1}{p}\cos(\theta+\widetilde{\alpha}_0)\,(2+q_1\cos\theta+q_2\sin\theta)+\frac{\varrho_2}{p} \tag{62b}$$
$$z_{\wp}(f) = \frac{\varrho_3}{p}\sin(\theta+\widetilde{\beta}_0) \tag{62c}$$

where,

$$\varrho_1 = \left(u_0^2+u_0'^2\right)^{1/2}$$
$$= \frac{a}{\eta}\left[\left(1-\eta^2\right)\delta\lambda_0^2+2\left(q_2\delta q_1-q_1\delta q_2\right)\delta\lambda_0-\left(q_1\delta q_1+q_2\delta q_2\right)^2+\delta q_1^2+\delta q_2^2\right]^{1/2} \tag{63a}$$
$$\varrho_2 = v_0(1+q_1\cos\theta_0+q_2\sin\theta_0)-u_0'(2+q_1\cos\theta_0+q_2\sin\theta_0)$$
$$= p\left[\delta\Omega\cos i+\frac{(1+\eta+\eta^2)}{\eta^3(1+\eta)}\left(q_2\delta q_1-q_1\delta q_2\right)+\frac{1}{\eta^3}\delta\lambda_0\right] \tag{63b}$$
$$\varrho_3 = \big[(1+2q_1\cos\theta_0+2q_2\sin\theta_0+q_1^2+q_2^2)w_0^2+(1+q_1\cos\theta_0+q_2\sin\theta_0)^2w_0'^2$$
$$-2\left(q_1\sin\theta-q_2\cos\theta\right)(1+q_1\cos\theta_0+q_2\sin\theta_0)w_0w_0'\big]^{1/2}$$
$$= p\left(\delta i^2+\delta\Omega^2\sin^2 i\right)^{1/2} \tag{63c}$$
$$\widetilde{\alpha}_0 = \tan^{-1}\left(\frac{u_0}{u_0'}\right)-\theta_0 = \tan^{-1}\left[\frac{(1+\eta)\left(\delta q_1+q_2\delta\lambda_0\right)-q_1\left(q_1\delta q_1+q_2\delta q_2\right)}{(1+\eta)\left(\delta q_2-q_1\delta\lambda_0\right)-q_2\left(q_1\delta q_1+q_2\delta q_2\right)}\right] \tag{63d}$$
$$\widetilde{\beta}_0 = \tan^{-1}\left(\frac{(1+q_1\cos\theta_0+q_2\sin\theta_0)w_0}{(1+q_1\cos\theta_0+q_2\sin\theta_0)w_0'-\left(q_1\sin\theta_0-q_2\cos\theta_0\right)w_0}\right)-\theta_0$$
$$= \tan^{-1}\left(-\frac{\delta\Omega\sin i}{\delta i}\right) \tag{63e}$$

Conversely, the orbital element differences δq_1, δq_2, and $\delta\lambda_0$ may be written in terms of the design parameters $\varrho_{1\ldots3}$, α_0, and β_0, as shown:

$$\delta q_1 = q_1q_2\frac{\varrho_1}{p}\cos\widetilde{\alpha}_0-(1-q_1^2)\frac{\varrho_1}{p}\sin\widetilde{\alpha}_0-q_2\left(\frac{\varrho_2}{p}-\delta\Omega\cos i\right) \tag{64a}$$
$$\delta q_2 = q_1q_2\frac{\varrho_1}{p}\sin\widetilde{\alpha}_0-(1-q_2^2)\frac{\varrho_1}{p}\cos\widetilde{\alpha}_0+q_1\left(\frac{\varrho_2}{p}-\delta\Omega\cos i\right) \tag{64b}$$

$$\delta\lambda_0 = \frac{\varrho_2}{p} - \delta\Omega\cos i - \frac{(1+\eta+\eta^2)}{(1+\eta)}\frac{\varrho_1}{p}\Big[q_1\cos\widetilde{\alpha}_0 - q_2\sin\widetilde{\alpha}_0\Big] \tag{64c}$$

It should be noted that though the use of nonsingular orbital elements eliminates problems with $e \to 0$, they are still not suitable for use when $i \to 0$. For example, $\cot i$ appears in Eqs. (61). Equinoctial elements[36] may be used to avoid this problem.

References

[1] Carpenter, J. R., Leitner, J. A., Folta, D. C., and Burns, R. D., "Benchmark Problems for Spacecraft Formation Flight Missions," *AIAA Guidance, Navigation, and Control Conference and Exhibit*, AIAA, Austin, TX, August 2003, AIAA-2003-5364.

[2] Curtis, S. A., "The Magnetosphere Multiscale Mission... Resolving Fundamental Processes in Space Plasmas," Tech. Rep. NASA TM-2000-209883, NASA Science and Technology Definition Team for the MMS Mission, 1999.

[3] Hill, G. W., "Researches in the Lunar Theory," *American Journal of Mathematics*, Vol. 1, No. 1, 1878, pp. 5–26.

[4] Clohessy, W. H. and Wiltshire, R. S., "Terminal Guidance System for Satellite Rendezvous," *Journal of the Aerospace Sciences*, Vol. 27, September 1960, pp. 653–658, 674.

[5] Knollman, G. C. and Pyron, B. O., "Relative Trajectories of Objects Ejected from a Near Satellite," *AIAA Journal*, Vol. 1, No. 2, February 1963, pp. 424–429.

[6] London, H. S., "Second Approximation to the Solution of Rendezvous Equations," *AIAA Journal*, Vol. 1, No. 7, July 1963, pp. 1691–1693.

[7] Karlgaard, C. D. and Lutze, F. H., "Second-Order Relative Motion Equations," *Journal of Guidance, Control, and Dynamics*, Vol. 26, No. 1, January-February 2003, pp. 41–49.

[8] Richardson, D. L. and Mitchell, J. W., "A Third-Order Analytical Solution for Relative Motion with a Circular Reference Orbit," *The Journal of the Astronautical Sciences*, Vol. 51, No. 1, January-March 2003, pp. 1–12.

[9] Anthony, M. L. and Sasaki, F. T., "Rendezvous Problem for Nearly Circular Orbits," *AIAA Journal*, Vol. 3, No. 9, September 1965, pp. 1666–1673.

[10] Kolemen, E. and Kasdin, N. J., "Relative Spacecraft Motion: A Hamiltonian Approach to Eccentricity Perturbations," *Advances in the Astronautical Sciences*, Vol. 119, No. 3, February 2004, pp. 3075–3086, also Paper AAS 04-294 of the AAS/AIAA Space Flight Mechanics Meeting.

[11] Kasdin, N. J. and Kolemen, E., "Bounded, Periodic Relative Motion using Canonical Epicyclic Orbital Elements," *Advances in the Astronautical Sciences*, Vol. 120, No. 2,

January 2005, pp. 3075–3086, also Paper AAS 05-186 of the AAS/AIAA Space Flight Mechanics Meeting.

[12] Vaddi, S. S., Vadali, S. R., and Alfriend, K. T., "Formation Flying: Accommodating Nonlinearity and Eccentricity Perturbations," *Journal of Guidance, Control, and Dynamics*, Vol. 26, No. 2, March-April 2003, pp. 214–223.

[13] Inalhan, G., Tillerson, M., and How, J. P., "Relative Dynamics and Control of Spacecraft Formations in Eccentric Orbits," *Journal of Guidance, Control, and Dynamics*, Vol. 25, No. 1, January-February 2002, pp. 48–59.

[14] Sengupta, P., Sharma, R., and Vadali, S. R., "Periodic Relative Motion Near a Keplerian Elliptic Orbit with Nonlinear Differential Gravity," *Journal of Guidance, Control, and Dynamics*, Vol. 29, No. 5, September-October 2006, pp. 1110–1121.

[15] Gurfil, P., "Relative Motion Between Elliptic Orbits: Generalized Boundedness Conditions and Optimal Formationkeeping," *Journal of Guidance, Control, and Dynamics*, Vol. 28, No. 4, July-August 2005, pp. 761–767.

[16] Melton, R. G., "Time Explicit Representation of Relative Motion Between Elliptical Orbits," *Journal of Guidance, Control, and Dynamics*, Vol. 23, No. 4, July-August 2000, pp. 604–610.

[17] Broucke, R. A., "Solution of the Elliptic Rendezvous Problem with the Time as Independent Variable," *Journal of Guidance, Control, and Dynamics*, Vol. 26, No. 4, July-August 2003, pp. 615–621.

[18] Wolfsberger, W., Weiß, J., and Rangnitt, D., "Strategies and Schemes for Rendezvous on Geostationary Transfer Orbit," *Acta Astronautica*, Vol. 10, No. 8, August 1983, pp. 527–538.

[19] Yamanaka, K. and Ankersen, F., "New State Transition Matrix for Relative Motion on an Arbitrary Elliptical Orbit," *Journal of Guidance, Control, and Dynamics*, Vol. 25, No. 1, January-February 2002, pp. 60–66.

[20] Tschauner, J. F. A. and Hempel, P. R., "Rendezvous zu einemin Elliptischer Bahn umlaufenden Ziel," *Astronautica Acta*, Vol. 11, No. 2, 1965, pp. 104–109.

[21] Sabol, C. A., McLaughlin, C. A., and Luu, K. K., "Meet the Cluster Orbits with Perturbations of Keplerian Elements (COWPOKE) Equations," *Advances in the Astronautical Sciences*, Vol. 114, No. 3, February 2003, pp. 573–594, also Paper AAS 03-138 of the AAS/AIAA Space Flight Mechanics Meeting.

[22] Sengupta, P., Vadali, S. R., and Alfriend, K. T., "Modeling and Control of Satellite Formations in High Eccentricity Orbits," *The Journal of the Astronautical Sciences*, Vol. 52, No. 1-2, January-June 2004, pp. 149–168.

[23] Battin, R. H., *An Introduction to the Mathematics and Methods of Astrodynamics*,

AIAA Education Series, American Institute of Aeronautics and Astronautics, Inc., Reston, VA, revised ed., 1999.

[24] Garrison, J. L., Gardner, T. G., and Axelrad, P., "Relative Motion in Highly Elliptical Orbits," *Advances in the Astronautical Sciences*, Vol. 89, No. 2, February 1995, pp. 1359–1376, also Paper AAS 95-194 of the AAS/AIAA Space Flight Mechanics Meeting.

[25] Alfriend, K. T., Schaub, H., and Gim, D.-W., "Gravitational Perturbations, Nonlinearity and Circular Orbit Assumption Effects on Formation Flying Control Strategies," *Advances in the Astronautical Sciences*, Vol. 104, February 2000, pp. 139–158, also Paper AAS 00-012 of the AAS Guidance and Control Conference.

[26] Vadali, S. R., Vaddi, S. S., and Alfriend, K. T., "A New Concept for Controlling Formation Flying Satellite Constellations," *Advances in the Astronautical Sciences*, Vol. 108, No. 2, February 2001, pp. 1631–1648, also Paper AAS 01-218 of the AAS/AIAA Space Flight Mechanics Meeting.

[27] Schaub, H., "Relative Orbit Geometry Through Classical Orbit Element Differences," *Journal of Guidance, Control, and Dynamics*, Vol. 27, No. 5, September-October 2004, pp. 839–848.

[28] Lane, C. M. and Axelrad, P., "Formation Design in Eccentric Orbits Using Linearized Equations of Relative Motion," *Journal of Guidance, Control, and Dynamics*, Vol. 29, No. 1, January-February 2006, pp. 146–160.

[29] Zanon, D. J. and Campbell, M. E., "Optimal Planner for Spacecraft Formations in Elliptical Orbits," *Journal of Guidance, Control, and Dynamics*, Vol. 29, No. 1, January-February 2006, pp. 161–171.

[30] Lawden, D. F., *Optimal Trajectories for Space Navigation*, Butterworths, London, UK, 2nd ed., 1963.

[31] Carter, T. E. and Humi, M., "Fuel-Optimal Rendezvous Near a Point in General Keplerian Orbit," *Journal of Guidance, Control, and Dynamics*, Vol. 10, No. 6, November-December 1987, pp. 567–573.

[32] Carter, T. E., "New Form for the Optimal Rendezvous Equations Near a Keplerian Orbit," *Journal of Guidance, Control, and Dynamics*, Vol. 13, No. 1, January-February 1990, pp. 183–186.

[33] Carter, T. E., "State Transition Matrices for Terminal Rendezvous Studies: Brief Survey and New Examples," *Journal of Guidance, Control, and Dynamics*, Vol. 21, No. 1, January-February 1998, pp. 148–155.

[34] Carpenter, J. R. and Alfriend, K. T., "Navigation Accuracy Guidelines for Orbital Formation Flying," *The Journal of the Astronautical Sciences*, Vol. 53, No. 2, April-June 2005, pp. 207–219.

[35] Vaddi, S. S., Alfriend, K. T., Vadali, S. R., and Sengupta, P., "Formation Establishment and Reconfiguration using Impulsive Control," *Journal of Guidance, Control, and Dynamics*, Vol. 28, No. 2, March-April 2005, pp. 262–268.

[36] Broucke, R. A. and Cefola, P. J., "On the Equinoctial Orbit Elements," *Celestial Mechanics*, Vol. 5, 1972, pp. 303–310.

List of Figure Captions

Figure 1: Frames of Reference

Figure 2: Effect of Bias Corrections on Along-Track Motion, $e = 0.6$

Figure 3: Near-PCO Relative Motion with HCW and Corrected Initial Conditions, $\varrho = 1\,\mathrm{km}$, $\alpha_0 = 0°$

a): $e = 0.2$

b): $e = 0.7$

Figure 4: Near-PCO Relative Motion with HCW and Corrected Initial Conditions, $\varrho = 1\,\mathrm{km}$, $\alpha_0 = 90°$

a): $e = 0.2$

b): $e = 0.7$

Figure 5: Effect of Eccentricity on Relative Orbit Plane

Figure 6: Near-GCO Relative Motion with HCW and Modified Initial Conditions, $e = 0.2$, $\varrho = 1\,\mathrm{km}$

a): $\alpha_0 = 0°$

b): $\alpha_0 = 90°$

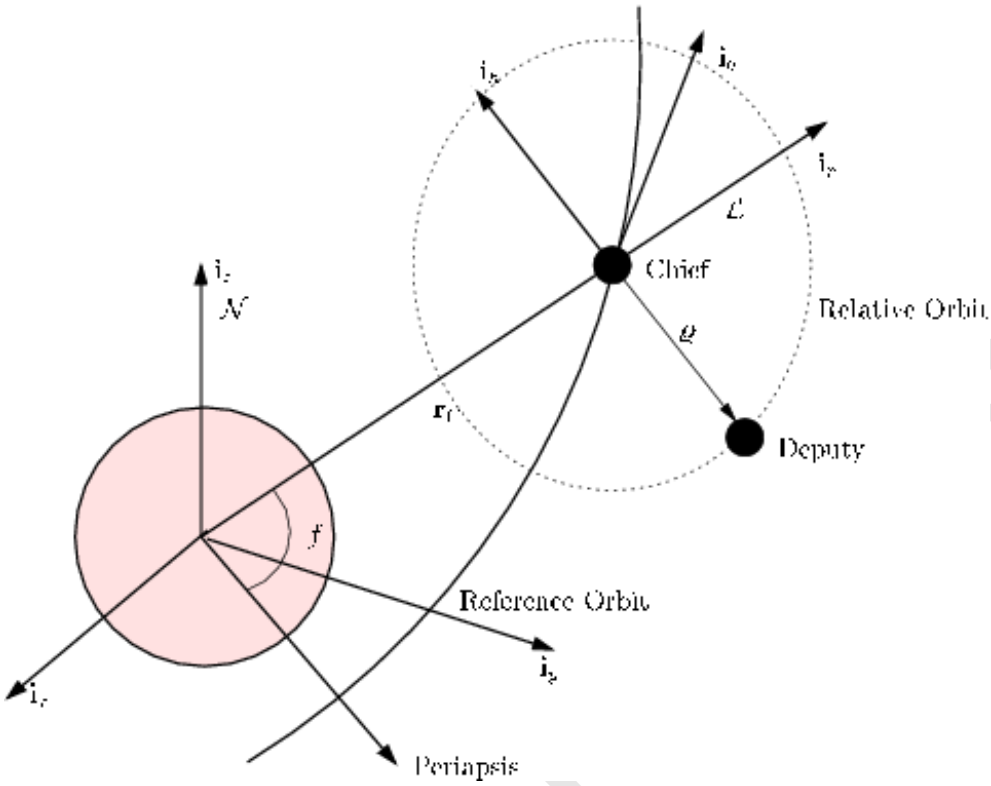

FIGURE 1:

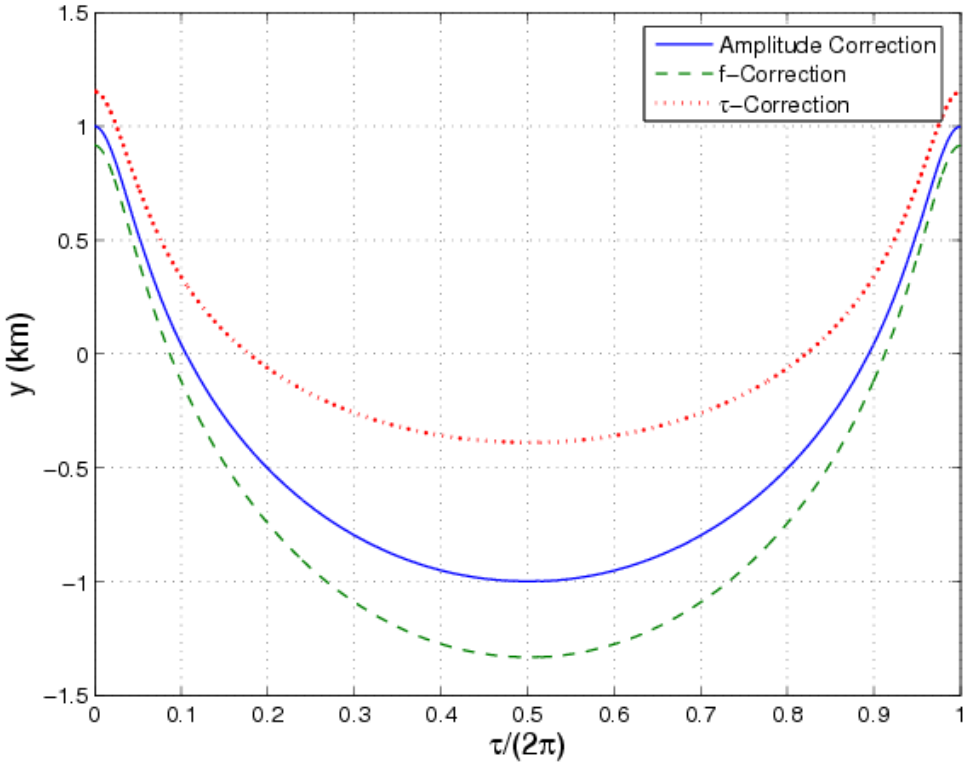

FIGURE 2:

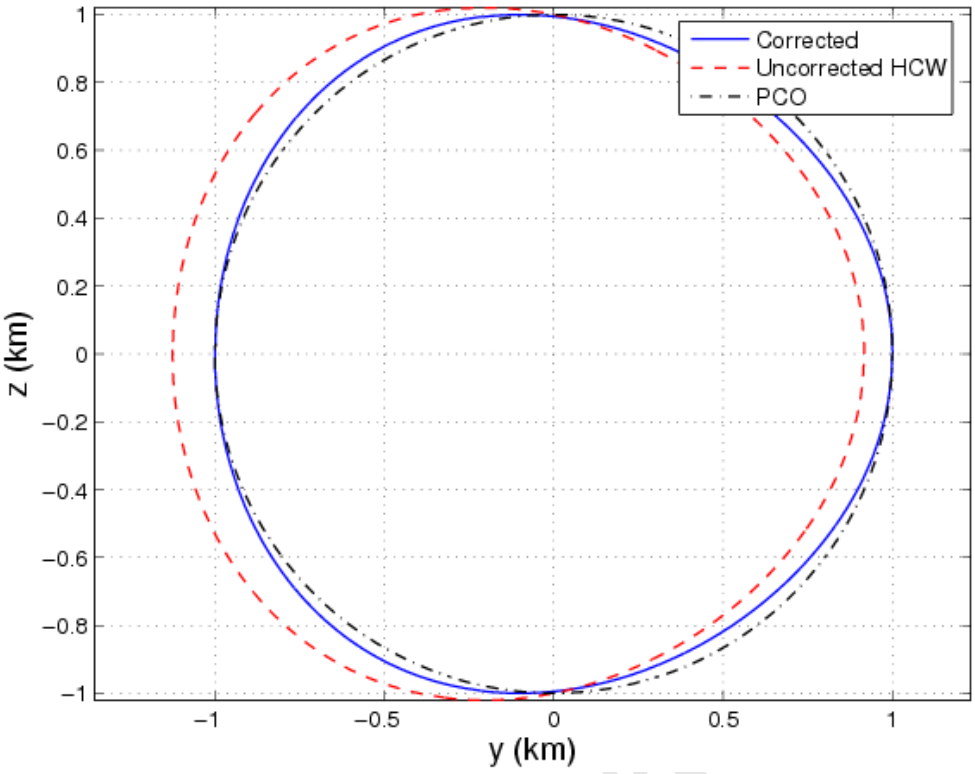

$e = 0.2$

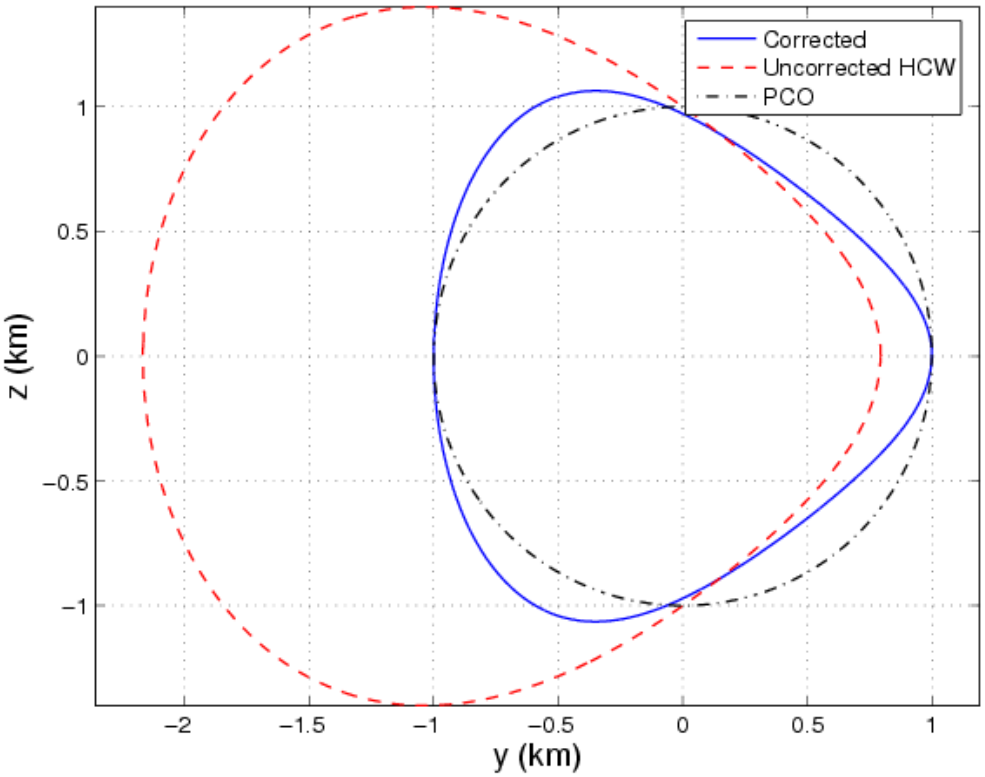

$e = 0.7$

FIGURE 3:

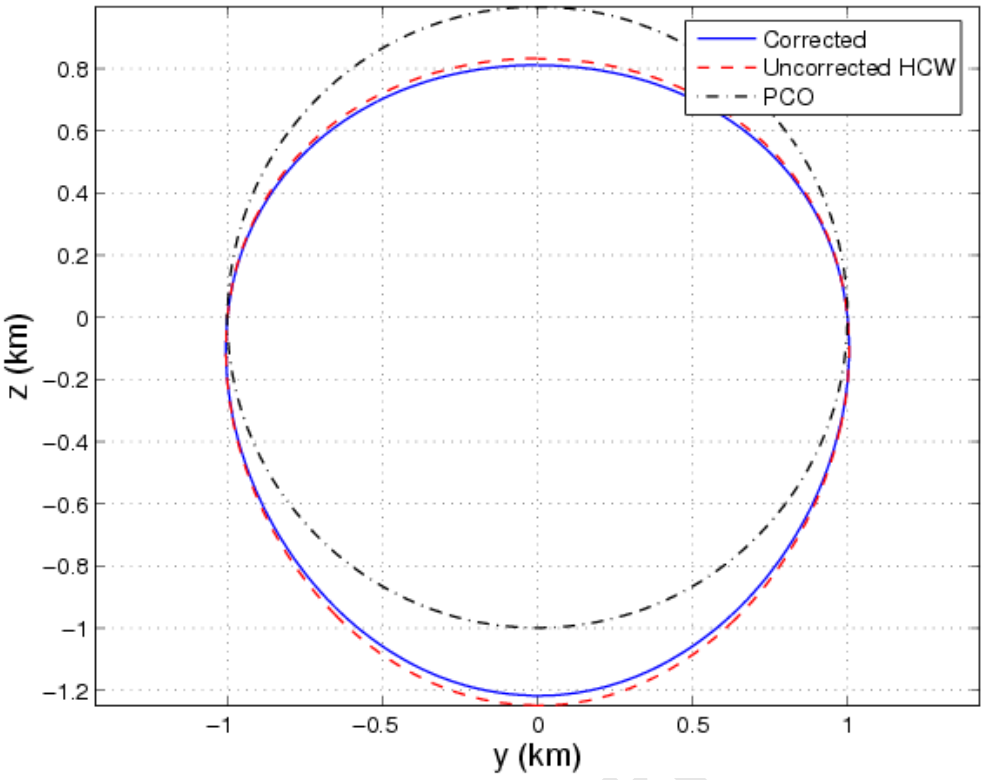

$e = 0.2$

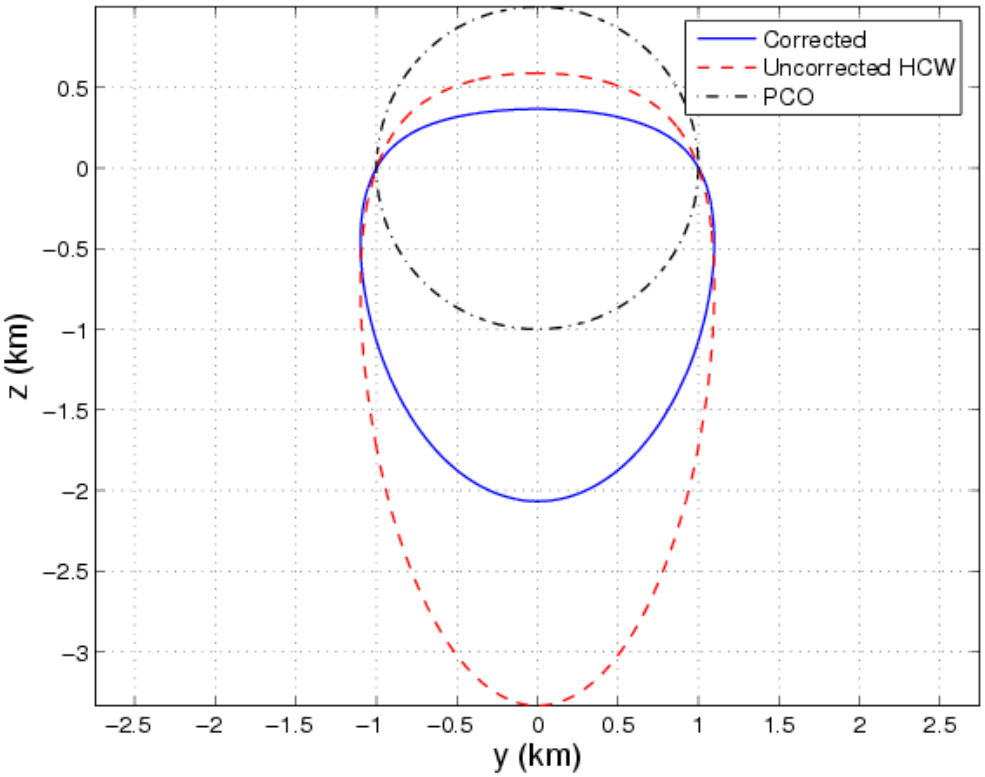

$e = 0.7$

FIGURE 4:

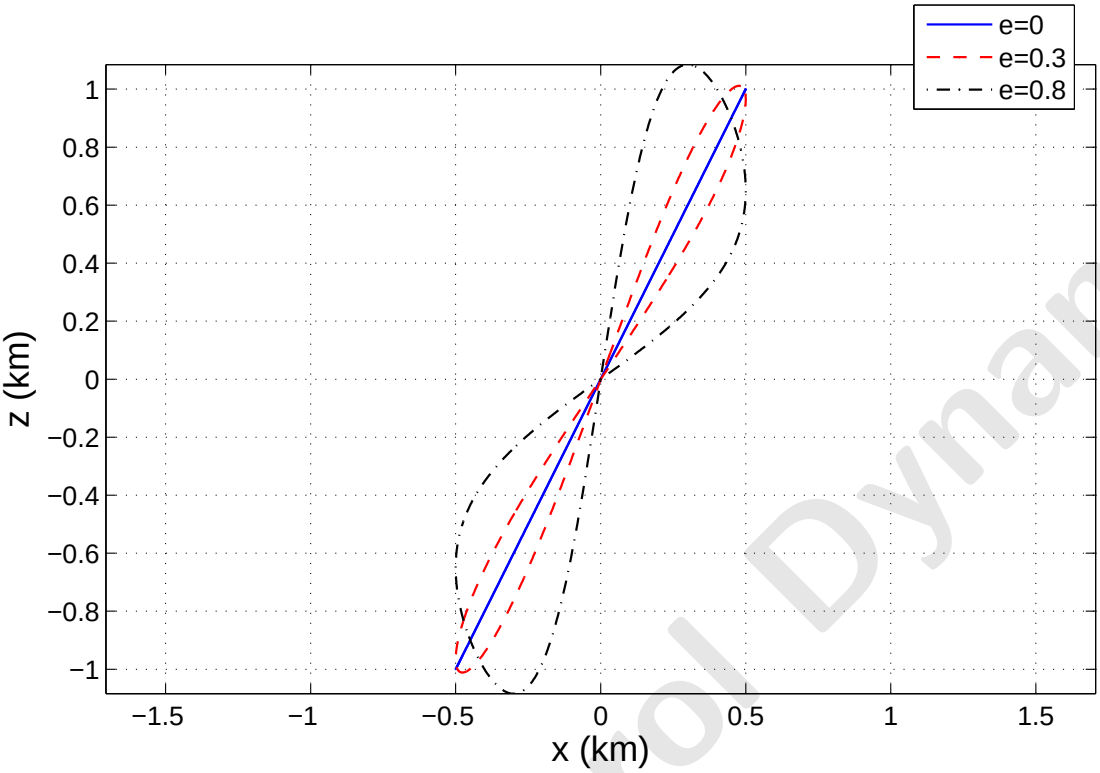

FIGURE 5:

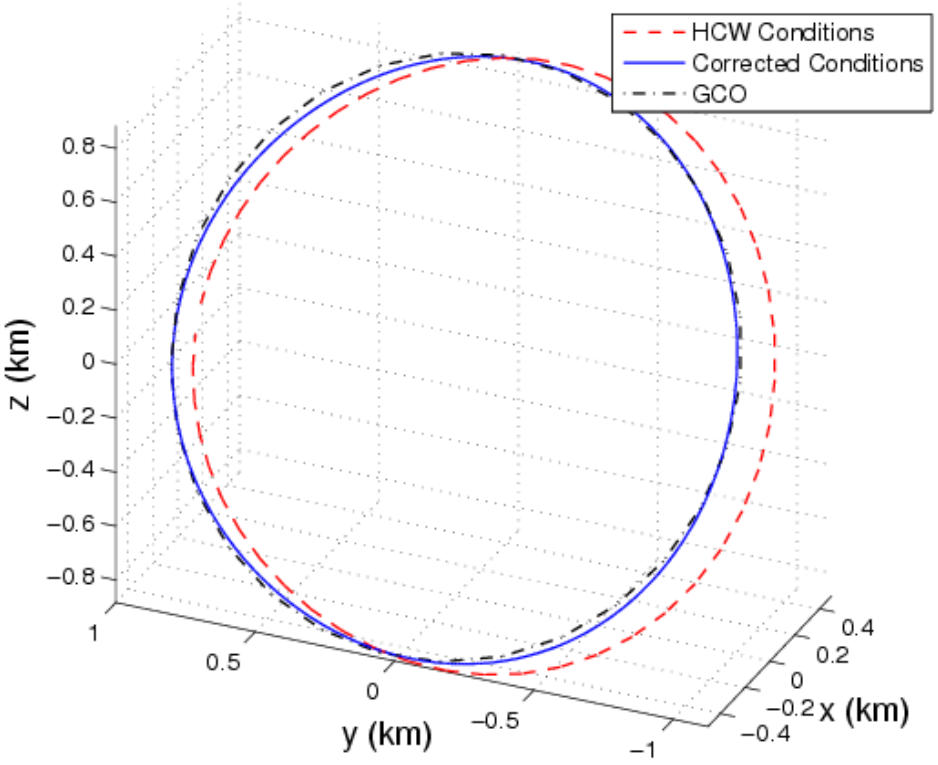

$\alpha_0 = 0°$

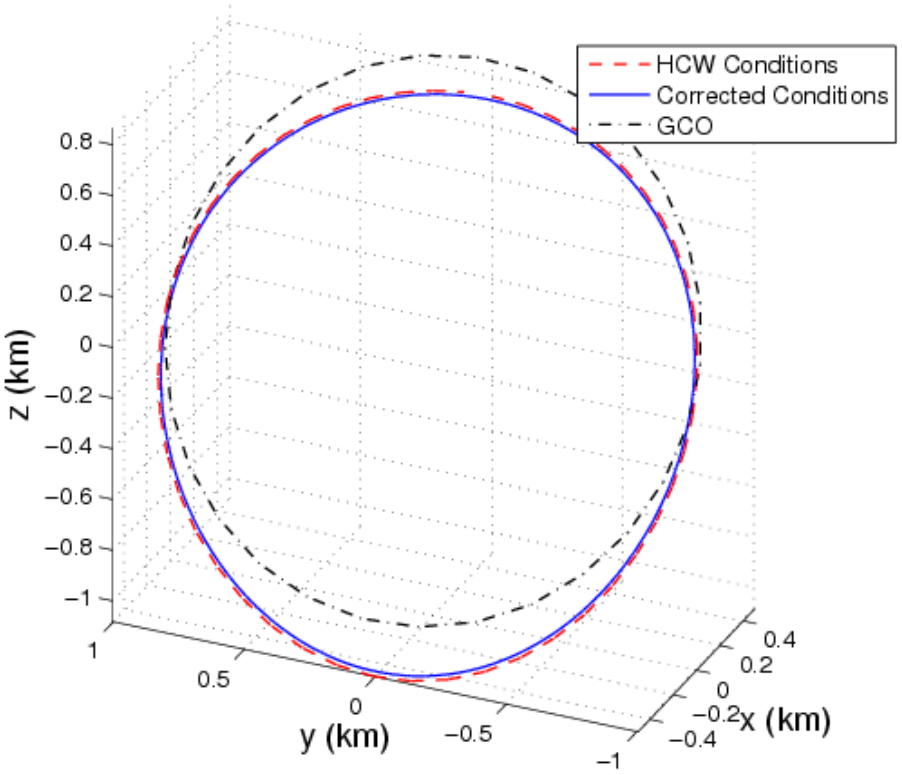

$\alpha_0 = 90°$

FIGURE 6: